Domain wall motion induced by the magnonic spin current

Xi-guang Wang, Guang-hua Guo,* Yao-zhuang Nie, Guang-fu Zhang, and Zhi-xiong Li
School of Physics Science and Technology, Central South University, Changsha, 410083, China
(Received 28 April 2012; revised manuscript received 17 August 2012; published 31 August 2012)

The spin-wave induced domain wall motion in a nanostrip with perpendicular magnetic anisotropy is studied. It is found that the domain wall can move either in the same direction or in the opposite direction to that of spin-wave propagation depending on whether the spin wave is reflected by the wall or transmitted through the wall. A magnonic momentum transfer mechanism is proposed and, together with the magnonic spin-transfer torque, a one-dimensional phenomenal model is constructed. The wall motion calculated based on this model is in qualitative agreement with micromagnetic simulations, showing that the model can describe the characteristics of spin-wave-induced wall motion and, especially, the wall motion direction.

DOI: 10.1103/PhysRevB.86.054445 PACS number(s): 75.60.Ch, 75.30.Ds, 75.40.Gb, 85.70.Kh

The magnetic domain wall motion induced by spin-transfer torque (STT) from a spin-polarized electrical current has attracted growing interest because of its fundamental relevance and potential applications in spintronic devices such as Racetrack memory and logic devices.[1–3] It is widely recognized that there are two types of STT acting on the wall when a spin-polarized current flows through it, namely the adiabatic STT and nonadiabatic STT.[4,5] The adiabatic STT comes from the adiabatic reversal of conduction electron spins, which induces a reaction torque on the wall as required by the conservation of angular momentum.[6] However, the origin of nonadiabatic STT still remains controversial. There are many contributions to this torque, such as spin-orbit interactions, spin-flip scattering, etc.[7–9] When the domain wall is narrow, the momentum transfer due to the electron reflection by the wall also contributes to the nonadiabatic STT.[10] The influence of the adiabatic and nonadiabatic STT on the wall motion is different. The adiabatic STT plays a more important role at the initial motion of the wall. It provides an initial velocity and causes the wall to move, but finally, it is balanced by an internal restoring torque and the wall motion ceases.[6] In contrast, the nonadiabatic STT behaves like a magnetic field and can sustain a steady-state wall motion.[5]

Recently, the noncharge-based spin current, magnonic spin current, is proposed[11] and experimentally demonstrated.[12] Similar to the spin-polarized electrical current, the magnonic spin current also leads to the STT in the magnet and can be exploited to control the spin structures, including the displacement of the domain wall. Hinzke *et al.*[13] first demonstrated theoretically that a single domain wall in a nanowire can be displaced by a magnonic spin current due to the temperature gradient. Yan *et al.*[14] showed that a spin wave excited by a microwave field can also drive a wall motion. They suggested that the mechanism of wall motion is the spin transfer torque resulting from the angular momentum transfer between the magnons and the local magnetization in the wall. As a magnon moves across the wall, its angular moment is changed by $2\hbar$ which is absorbed by the wall, making the wall propagate in the opposite direction to that of the magnon. It is worth noting that the spin-wave-induced domain wall motion was studied earlier in Refs. 15–17. By micromagnetic simulations, the authors noticed that, contrary to the result in Refs. 13 and 14, the spin wave causes the wall to move in the same direction to that of spin-wave propagation, and the wall velocity is strongly dependent on the transmission coefficient of spin wave. So far, there is no theory to explain the wall motion induced by spin waves.

In this letter, by using micromagnetic simulations, we study a single 180° Bloch domain wall motion induced by spin waves in a nanostrip with perpendicular magnetic anisotropy (PMA). It is found that the direction and velocity of wall motion are strongly dependent on the spin-wave frequency. In the high-frequency region, where the transmission coefficient of spin waves passing through the wall is very close to a unit, the wall moves in the opposite direction to that of magnons. While in the low-frequency region, an obvious reflection of spin waves occurs. In this case, the wall propagates in the same direction to that of incident magnons, and its velocity increases with the decrease in the spin-wave frequency. In order to explain the characteristics of spin-wave-induced wall motion, we propose a magnonic momentum transfer mechanism and construct a one-dimensional phenomenological model to account for the simulation results.

The PMA nanostrip studied here is 6 μm long in the x direction, 50 nm wide in the y direction, and 10 nm thick in the z direction, as shown in Fig. 1. For micromagnetic simulation, the following material parameters are used: saturation magnetization $M_s = 8.6 \times 10^5$ A/m, exchange stiffness $A_{ex} = 1.3 \times 10^{-11}$ J/m, perpendicular anisotropy constant $K_1 = 5.8 \times 10^5$ J/m^3 and Gilbert damping constant $\alpha = 0.01$. Micromagnetic simulations presented here are performed with the micromagnetic code of OOMMF.[18] The simulation cell size is chosen to be $2 \times 2 \times 10$ nm^3. No thermal effects are considered. A 180° Bloch wall is placed at the center position ($X = 0$) and relaxed to stable. The wall width is $\delta = \pi\Delta = 19.1$ nm. An external harmonic sinusoidal field $H = H_0 \sin(2\pi v_H t)\hat{y}$ along the y axis is applied locally in an area ($2 \times 50 \times 10$ nm^3) in the left side of the strip to excite spin waves, which propagates along the nanostrip and induces the wall to move.

The displacements of the wall driven by the spin wave with frequencies of 70 and 22 GHz are shown in Fig. 2. For the spin wave with frequency $f = 70$ GHz [Fig. 2(b)], the wall moves in the opposite direction to that of the magnon, and its speed is almost constant. This result is in agreement with Ref. 14. However, for the spin wave of frequency

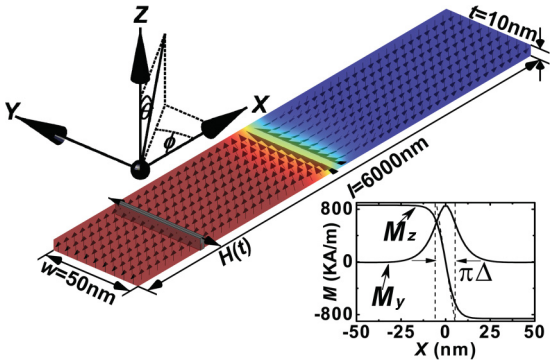

FIG. 1. (Color online) Illustration of the Model PMA nanostrip with the geometry and dimensions. A 180° Bloch domain wall is positioned at the center $X = 0$. The magnetization direction is represented by arrows. The gray area with $H(t)$ represents the region where spin waves are excited. The Cartesian coordinate system is shown on the higher left. The lower right inset shows the magnetization components of the wall profiles.

$f = 22$ GHz [Fig. 2(a)], the situation appears to be quite different. The domain wall moves in the same direction to that of the spin-wave propagation and displays a complicated behavior. At first, the wall moves with an acceleration stage, and then it enters into a relatively steady-state motion with an almost constant velocity (denoted as v_s). Finally, the wall velocity decreases as it moves gradually away from the exciting region.

Figure 3(a) shows the frequency dependence of wall velocity. In the case that the wall moves in the same direction to that of the spin-wave propagation, this velocity corresponds to the steady-state motion v_s. Considering that the efficiency of spin-wave excitation is strongly dependent on the frequency of the microwave field as indicated by Fig. 4, the velocity is normalized by $(\rho/M_s)^2$ for comparison, where ρ is the amplitude of spin waves. It shows that the wall velocity decreases rapidly with the increase in frequency. In the

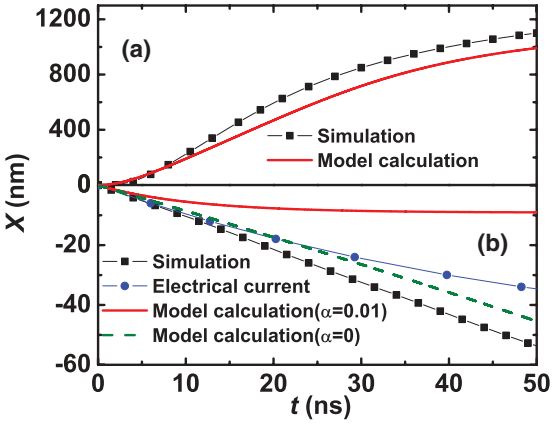

FIG. 2. (Color online) The wall displacement X as a function of time t, induced by propagating spin waves of frequency (a) 22 GHz and (b) 70 GHz. The black squares are the micromagnetic simulation results. The red solid line and green dashed line represent the model calculation with $\alpha = 0.01$ and 0, respectively. The blue circle is the simulation results of wall motion driven by the equivalent spin-polarized electrical current.

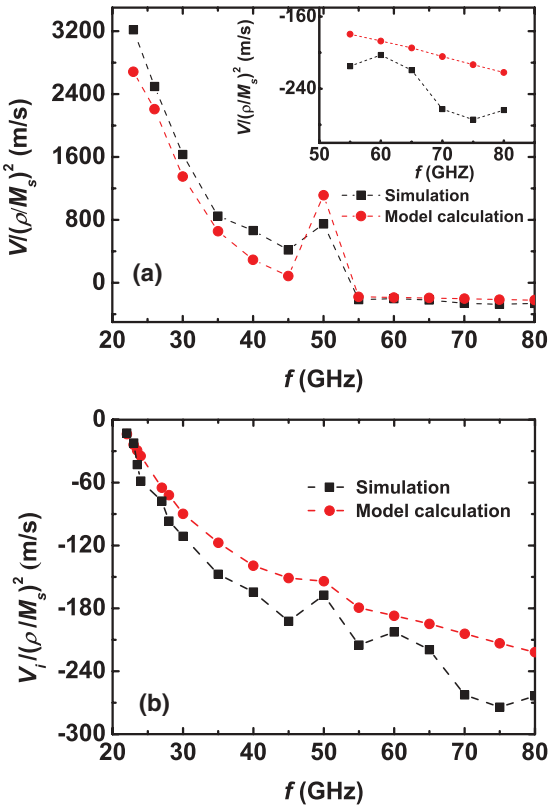

FIG. 3. (Color online) (a) Simulated (black squares) and model calculated (red circles) wall velocity v and (b) initial wall velocity v_i as a function of the frequency. The amplified scale of the wall velocity induced by the spin wave with frequencies larger than 55 GHz is shown as an inset of (a). All the velocities are normalized by $(\rho/M_s)^2$. The dashed lines are guides for the eye.

low-frequency region, the wall moves in the same direction to that of the spin wave ($v > 0$). At a frequency of about 50 GHz, there is a sudden increase in the velocity compared with neighboring frequencies. For frequencies larger than 55 GHz, the velocity becomes negative ($v < 0$) as indicated by the inset of Fig. 3(a), meaning that the spin wave drags the wall to the opposite direction. It should be mentioned that the actual maximum value of the speed is approximately 40 m/s, and Walker breakdown is not observed in the range of our simulation.

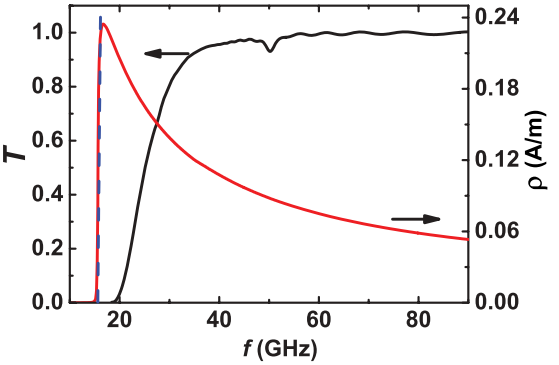

FIG. 4. (Color online) Transmission coefficient T of spin wave passing through the domain wall (black solid line) and amplitude of spin wave ρ (red/dark gray solid line) as a function of the frequency.

In order to understand the above results, we calculated the frequency dependences of the spin-wave amplitude ρ and the transmission coefficients T passing through the domain wall, which are shown in Fig. 4. For calculations, a sinc function field $H_0 \sin(2\pi v_H t)/(2\pi v_H t)\hat{y}$ with $H_0 = 3$ mT and $v_H = 150$ GHz is used. Thus, spin waves of frequencies from 0 to 150 GHz can be excited. Spin waves having frequencies lower than 18 GHz are prohibited to propagate in the nanostrip. It can be seen from Fig. 4 that the amplitude ρ decreases with the increase in frequency. The transmission coefficients T are also sensitively dependent on the frequency. In the region of frequencies larger than 55 GHz, the spin waves pass through the domain wall without reflection. For frequencies lower than 55 GHz, the spin waves are partially reflected, and the transmission coefficients decrease with frequency. It has been established that, for a one-dimensional domain wall, a spin wave can be transmitted without reflection,[19,20] but for the wall in nanostrip, partial or complete reflection of a spin wave may occur when the wavelength is larger than the wall width.[21] The reflective behavior results from the stray field due to the transversely confined dimension. Also, the reflectivity is also related to the inherent oscillation modes of the wall.[15] This is displayed on our $T(f)$ curve as well, where at frequencies of about 50 GHz, there is a clearly drop of transmission. This drop corresponds to a normal oscillation mode of the wall.

Therefore, it is clearly shown that, for the 180° Bloch domain wall in PMA nanostrips, the spin-wave-induced wall motion exhibits different behaviors depending on whether the spin wave passes through the wall or it is reflected by the wall. Very recently, Kim *et al.* studied the spin-wave-induced Néel-wall motion in a nanostrip by using micromagnetic simulations.[22] They also found that the wall velocity is strongly dependent on the spin-wave frequency. At certain frequencies, the wall velocity is negative, while at other frequencies where strong spin-wave reflection occurs, the wall has a positive velocity. Moreover, the internal normal oscillation modes of the wall also influence the wall motion. According to our studies, the wall motion direction is determined by the transmission or reflection characteristics of a spin wave. When the spin-wave frequency is the same as that of an internal mode of the wall, the resonant reflection occurs and acts on the wall motion.

Hinzke *et al.*[13] and Yan *et al.*[14] have proposed a magnonic spin-transfer torque mechanism to explain the spin-wave-induced wall motion. When a magnon passes through the wall, its spin is adiabatically reversed, and this induces a reaction torque on the wall as required by the conservation of angular momentum, which makes the wall propagate in the opposite direction to that of the magnon. Obviously, this mechanism cannot explain the feature of wall motion when a spin wave is reflected by the wall. In the case that a magnon is reflected, its spin keeps constant, but its momentum is changed by $2\hbar k$. Here, k is the wave vector of the spin wave. The transfer of momentum between the magnon and the wall also induces torque acting on the wall and pushes it moving in the same direction to that of the incident magnon. This type of momentum transfer torque was proposed by Tatara *et al.*[10] regarding the spin-polarized electrical-current-induced nonadiabatic STT.

In the following, we will establish a one-dimensional phenomenological model to account for the spin-wave-induced wall motion by introducing the above-mentioned magnonic spin transfer torque and momentum transfer torque of magnonic currents. When a magnonic current passes through a domain wall, the magnon spin, which is opposite to local magnetization, is adiabatically reversed.[13,14] Similar to the spin-polarized current, an magnonic STT is brought out, which can be expressed in a one-dimensional situation as:[23]

$$\left(\frac{\partial \vec{M}}{\partial t}\right)_{\mathrm{ST}} = -\frac{\partial \vec{J}_m}{\partial x}. \tag{1}$$

Here, $\vec{J}_m = -u\vec{M}$. The negative sign means that the magnon spin is antiparallel to the direction of the local magnetization. Here, $u = (\gamma \hbar n v_k)/\mu_o M_s$, n is the number of magnons per unit area, v_k is the propagation velocity of magnons, and $\gamma = \mu_0 g e/2m_e$ represents the gyromagnetic ratio. In the case that the magnonic current is reflected completely by the wall, the momentum transfer between the magnons and the wall gives rise to a force $F = dP_{\mathrm{magnon}}/dt = 2nv_k\hbar k$, which pushes the wall to move forward. We can introduce an effective field $H_{\mathrm{magnon}} = (nv_k\hbar k)/(\mu_0 M_s) = uk/\gamma$ along the direction perpendicular to the nanostrip to describe this momentum transfer mechanism.

By assuming a constant domain wall profile, the wall dynamics can be described by two collective coordinates, the wall position X and the tilt angle φ of the wall magnetization.[24,25] For a one-dimensional Bloch wall profile, the equations of wall motion including the spin-wave induced torques become

$$(1+\alpha^2)\dot{X} = \frac{\gamma \Delta K_d}{\mu_0 M_s}\sin(2\varphi) - Tu + (1-T)\alpha\Delta uk, \tag{2}$$

$$(1+\alpha^2)\dot{\varphi} = -\frac{\gamma\alpha K_d}{\mu_0 M_s}\sin(2\varphi) + (1-T)uk + T\frac{\alpha u}{\Delta}. \tag{3}$$

Here, $K_d = \frac{1}{2}\mu_0 M_s^2(N_x - N_y)$ is the effective anisotropy, representing the magnetostatic energy difference between the Bloch wall and the Néel wall,[26] where N_x and N_y are the demagnetizing factors along the x and y directions, respectively. Also, $N_x - N_y$ is calculated to be 0.05, and T is the transmission coefficient of spin waves passing through the wall. The initial wall velocity corresponding to the condition $\varphi = \pi/2$ can be derived from Eq. (2) as:

$$v_i = -\frac{T}{1+\alpha^2}u + \frac{(1-T)\alpha\Delta k}{1+\alpha^2}u. \tag{4}$$

Equation (4) clearly indicates that transmitted magnons drag the wall to move backward, and the reflected magnons drive the wall to propagate forward with respect to the propagation direction of spin waves. As the damping constant $\alpha \ll 1$, the initial wall velocity is mainly determined by the first term. After the initial acceleration motion, the wall enters into a steady-state motion corresponding to the condition $\partial\varphi/\partial t = 0$. The steady-state motion velocity can be expressed as the following:

$$v_s = \frac{(1-T)\Delta k}{\alpha}u. \tag{5}$$

The above formula shows that v_s is determined by the reflected magnons, which transfer their linear momentum to the wall and push it to move.

For numerical calculations of wall position $X(t)$, initial velocity v_i as well as steady-state motion velocity v_s, the magnon density n must be decided at first. Here, n is directly proportional to the square of the spin-wave amplitude, which can be approximated as $n = \rho^2/(2M_s g\mu_B)$,[27] where ρ is the spin-wave amplitude. The transmission coefficient T, spin-wave amplitude ρ, wave vector k, and velocity v_k, which are all functions of the spin-wave frequency, are taken from the micromagnetic simulation results. Also, ρ is a function of wall position because of the gradual attenuation of the spin wave as it propagates away from exciting source.

The wall displacements calculated from the above one-dimensional model are depicted in Fig. 2 together with the data obtained by micromagnetic simulations. For a spin wave with $f = 22$ GHz [see Fig. 2(a)], the $X(t)$ curve calculated based on the one-dimensional model is in qualitative agreement with the simulation results. The wall motion can be classified into three phases: initial acceleration motion, a relatively steady-state motion, and finally, the gradual deceleration motion, but for a spin wave with frequency $f = 70$ GHz [see Fig. 2(b)], there is a large difference between the theoretically calculated results and micromagnetic simulation data. In the case of the theoretical calculation, the wall moves a certain distance and then ceases to move. To shed more light on this difference, we simulate the wall motion driven by the adiabatic STT of spin-polarized electrical currents. The strength of this STT is the same value as the magnon's. As the adiabatic STT of spin-polarized electrical currents is $\tau_e = -u_e \frac{\partial \vec{M}}{\partial x}$, this gives the equivalent value $u_e = u = (\gamma \hbar n v_k)/\mu_o M_s$. Here, we get a similar result as that of the simulated spin-wave-induced wall motion; the wall moves a much longer distance compared to the one-dimensional model calculation. This illuminates that the difference between the simulated and model-calculated data mainly results from the one-dimensional approximation of wall motion. In addition, the wall motion induced by the magnonic STT is sensitive to the damping constant α, as indicated by Fig. 2.

The initial wall velocity v_i as well as velocity v_s in the steady-state motion vs the frequency of spin waves calculated from Eqs. (4) and (5) are shown in Figs. 3(b) and 3(a), respectively, together with the simulated data. It can be seen that the analytical results are in qualitative agreement with the simulation. The initial v_i increases with the frequency. As indicated by Eq. (4), v_i is mainly determined by the magnons passing through the wall. The transmission coefficient T and the spin velocity v_k all lead v_i to increase with the frequency. It is worth noting that v_i is much lower than v_s, meaning the reflected magnons can give rise to a larger torque on the wall than the transmitted magnons. This can be understood from Eqs. (4) and (5) that $v_s/v_i \approx (1 + \alpha^2)\Delta k/\alpha$ when the same number of magnons is reflected or passing through the wall. Taking $k = 1 \times 10^8$ m^{-1} gives $v_s/v_i \approx 61$.

In conclusion, we have studied a Bloch domain wall motion in a PMA nanostrip induced by spin waves (or magnonic currents). It is demonstrated that the behavior of the wall motion is strongly dependent on whether the magnons pass through the wall or they are reflected by the wall. When the magnons pass through the wall, the spin transfer torque, which originates from the spin transfer between the magnons and the wall, makes the wall propagate in the opposite direction to that of the magnons. When the magnons are reflected by the wall, the momentum transfer between the magnons and the wall also gives rise to torque, which drives the wall to move in the same direction to that of the incident magnons. By controlling the transmission coefficient of the spin wave, the wall motion velocity as well as direction can be manipulated. The results obtained in this work may find their use in designing magnonic spin devices.

ACKNOWLEDGMENTS

This work was supported by the National Natural Science Foundation of China under Grant No. 60571043, Doctoral Fund of Ministry of Education of China, and the Scientific Plane Project of Hunan Province of China under Grant No. 2011FJ3193.

*Corresponding author: guogh@mail.csu.edu.cn

[1] D. A. Allwood, G. Xiong, C. C. Faulkner, D. Atkinson, D. Petit, and R. P. Cowburn, Science **309**, 1688 (2005).
[2] M. Hayashi, L. Thomas, R. Moriya, C. Rettner, and S. S. P. Parkin, Science **320**, 209 (2008).
[3] S. S. P. Parkin, M. Hayashi, and L. Thomas, Science **320**, 190 (2008).
[4] S. Zhang and Z. Li, Phys. Rev. Lett. **93**, 127204 (2004).
[5] A. Thiaville, Y. Nakatani, J. Miltat, and Y. Suzuki, Europhys. Lett. **69**, 990 (2005).
[6] Z. Li and S. Zhang, Phys. Rev. B **70**, 024417 (2004).
[7] I. Garate, K. Gilmore, M. D. Stiles, and A. H. MacDonald, Phys. Rev. B **79**, 104416 (2009).
[8] R. A. Duine, A. S. Núñez, J. Sinova, and A. H. MacDonald, Phys. Rev. B **75**, 214420 (2007).
[9] P. Baláž, V. K. Dugaev, and J. Barnaś, Phys. Rev. B **85**, 024416 (2012).
[10] G. Tatara and H. Kohno, Phys. Rev. Lett. **92**, 086601 (2004).
[11] Y. Kajiwara, K. Harii, S. Takahashi, J. Ohe, K. Uchida, M. Mizuguchi, H. Umezawa, H. Kawai, K. Ando, K. Takanashi, S. Maekawa, and E. Saitoh, Nature (London) **464**, 262 (2010).
[12] A. V. Chumak, A. A. Serga, M. B. Jungfleisch, R. Neb, D. A. Bozhko, V. S. Tiberkevich, and B. Hillebrands, Appl. Phys. Lett. **100**, 082405 (2012).
[13] D. Hinzke and U. Nowak, Phys. Rev. Lett. **107**, 027205 (2011).
[14] P. Yan, X. S. Wang, and X. R. Wang, Phys. Rev. Lett. **107**, 177207 (2011).
[15] D. S. Han, S. K. Kim, J. Y. Lee, S. J. Hermsdoerfer, H. Schultheiss, B. Leven, and B. Hillebrands, Appl. Phys. Lett. **94**, 112502 (2009).

[16]M. Jamali, H. Yang, and K. J. Lee, Appl. Phys. Lett. **96**, 242501 (2010).
[17]S. M. Seo, H. W. Lee, H. Kohno, and K. J. Lee, Appl. Phys. Lett. **98**, 012514 (2011).
[18]M. J. Donahue and D. G. Porter, The Object Oriented MicroMagnetic Framework (OOMMF) project at ITL/NIST, http://math.nist.gov/oommf/.
[19]A. A. Thiele, Phys. Rev. B **7**, 391 (1973).
[20]C. Bayer, H. Schultheiss, B. Hillebrands, and R. L. Stamps, IEEE Trans. Magn. **41**, 3094 (2005).
[21]S. Macke and D. Goll, J. Phys.: Conf. Ser. **200**, 042015 (2010).
[22]J. S. Kim, M. Stärk, M. Kläui, J. Yoon, C. Y. You, L. Lopez-Diaz, and E. Martinez, Phys. Rev. B **85**, 174428 (2012).
[23]J. Fernández-Rossier, M. Braun, A. S. Núñez, and A. H. MacDonald, Phys. Rev. B **69**, 174412 (2004).
[24]N. L. Schryer and L. R. Walker, J. Appl. Phys. **45**, 5406 (1974).
[25]L. Thomas, M. Hayashi, X. Jiang, R. Moriya, C. Rettner, and S. S. P. Parkin, Nature (London) **443**, 197 (2006).
[26]S. W. Jung, W. Kim, T. D. Lee, K. J. Lee, and H. W. Lee, Appl. Phys. Lett. **92**, 202508 (2008).
[27]A. G. Gurevich and G. A. Melkov, *Magnetization Oscillations and Waves* (CRC, New York, 1996).